Correlative relationship between nanomorphology, crystallinity, texture and device efficiency of organic BHJ solar cells studied by energy-filtered TEM

Christina Harreiss[1], Mingjian Wu[2], Stefan Langner[3], Stefanie Rechberger[4], Johannes Will[4], Christoph J. Brabec[3] and Erdmann Spiecker[2]

[1]Institute of Micro- and Nanostructure Research (IMN) & Center for Nanoanalysis and Electron Microscopy (CENEM), Interdisciplinary Center for Nanostructured Films (IZNF), Department of Materials Science and Engineering, Friedrich-Alexander University Erlangen-Nürnberg (FAU), Erlangen, Germany, Bayern, Germany, [2]Institute of Micro- and Nanostructure Research (IMN) & Center for Nanoanalysis and Electron Microscopy (CENEM), Interdisciplinary Center for Nanostructured Films (IZNF), Department of Materials Science and Engineering, Friedrich-Alexander University Erlangen-Nürnberg (FAU), Erlangen, Germany, Erlangen, Bayern, Germany, [3]Institute of Materials for Electronics and Energy Technology (i-MEET), Department of Materials Science and Engineering, Friedrich-Alexander University Erlangen-Nürnberg (FAU), Erlangen, Germany, Germany, [4]Institute of Micro- and Nanostructure Research (IMN) & Center for Nanoanalysis and Electron Microscopy (CENEM), Interdisciplinary Center for Nanostructured Films (IZNF), Department of Materials Science and Engineering, Friedrich-Alexander University Erlangen-Nürnberg (FAU), Erlangen, Germany, Germany

Solution-processed bulk heterojunction (BHJ) solar cells based on a polymeric or small molecule electron donor and a fullerene derivative as electron acceptor are already well known in organic photovoltaic (OPV) research since more than 20 years.[1] However, an in-depth knowledge on the interplay between the underlying nanostructure of the active layer and the device performance is still missing. Understanding and controlling the nanomorphology is of high importance since it determines the exciton diffusion and dissociation at the donor-acceptor interface as well as the charge carrier separation and transportation to the respective electrode, which decisively influences the device efficiency of the solar cell. The device performance can be highly improved by post-processing routines like solvent vapor (SVA) and thermal annealing (TA) which enable tailoring the nanomorphology evolution during the respective treatment.[2]

Here, we studied the effects of SVA and TA on a high-efficiency photovoltaic system composed of a small molecule 2,2'-[(3,3''',3'''',4'-tetraoctyl[2,2':5',2'':5'',2''':5''',2''''-quinquethiophene]-5,5''''-diyl)bis[(Z)-methylidyne(3-ethyl-4-oxo-5,2-thiazolidinediylidene)]]bis-propanedinitrile (DRCN5T) electron donor and [6,6]-phenyl C71 butyric acid methyl ester ($PC_{71}BM$) as electron acceptor by *in situ* as well as *ex situ* energy-filtered transmission electron microscopy (EFTEM) techniques. This approach enables the discrimination between electron donor and electron acceptor phases visualizing and revealing the material distribution of both components. For the SVA process, we investigated the interplay between nanostructure, crystallinity, texture and device performance as a function of the annealing solvent as well as the annealing time. Four different solvent vapor atmospheres were applied ($CHCl_3$, THF, CS_2 and $C_3H_6O_2$) demonstrating various solubilities for DRCN5T and $PC_{71}BM$. Our systematic EFTEM study on the nanomorphology evolution revealed a clear dependence on the applied annealing solvent. Different types of nanomorphologies and various states of fiber growth were obtained as a function of the annealing solvent and annealing time. However, independent of the choice of the solvent an optimal donor domain size with same dimensions was revealed that occurred for all annealing solvents at different annealing times. This exhibits a clear correlation between the solvent solubility and the underlying kinetics of phase separation and fiber growth. At the optimal donor domain size, the highest device efficiency was obtained in all four cases. Furthermore, an optimal crystal coherence length (CCL) of the DRCN5T crystals as well

as a preferred orientation of the crystallites can be identified by energy-filtered electron diffraction (EF-ED) analyses and diffraction imaging (i.e. nano-beam 4D-STEM) methods[3], respectively (Figure 1). Bringing all the findings together, we can now predict the optimal annealing time resulting in the highest power conversion efficiency (PCE) for any solvent with known solubility.

To gain a better understanding of the phase formation, thermal annealing experiments were performed *in situ* in the TEM using two different TEM heating holders (conventional heating holder and MEMS-based heating holder). Thus, phase separation and fiber growth processes could be studied in real time during the thermal treatment. We applied various annealing temperatures between 80°C and 160°C and observed the nanomorphology and crystallinity evolution as a function of the annealing time. Here, a clear dependence of the annealing temperature on the speed of phase separation and fiber growth could be revealed. In addition, an Arrhenius plot could be generated from the individual growth rates and an activation energy E_A of 55 kJ/mol is obtained. Even though stepwise heating was performed in the conventional heating holder in comparison to direct heating in the MEMS-based system, both approaches delivered similar results. Investigations on the evolution of the crystallinity demonstrate a continuous growth of the DRCN5T crystals as a function of the annealing temperature. Furthermore, we figured out that the preferred crystal orientation is changing with increasing annealing temperatures (Figure 2).
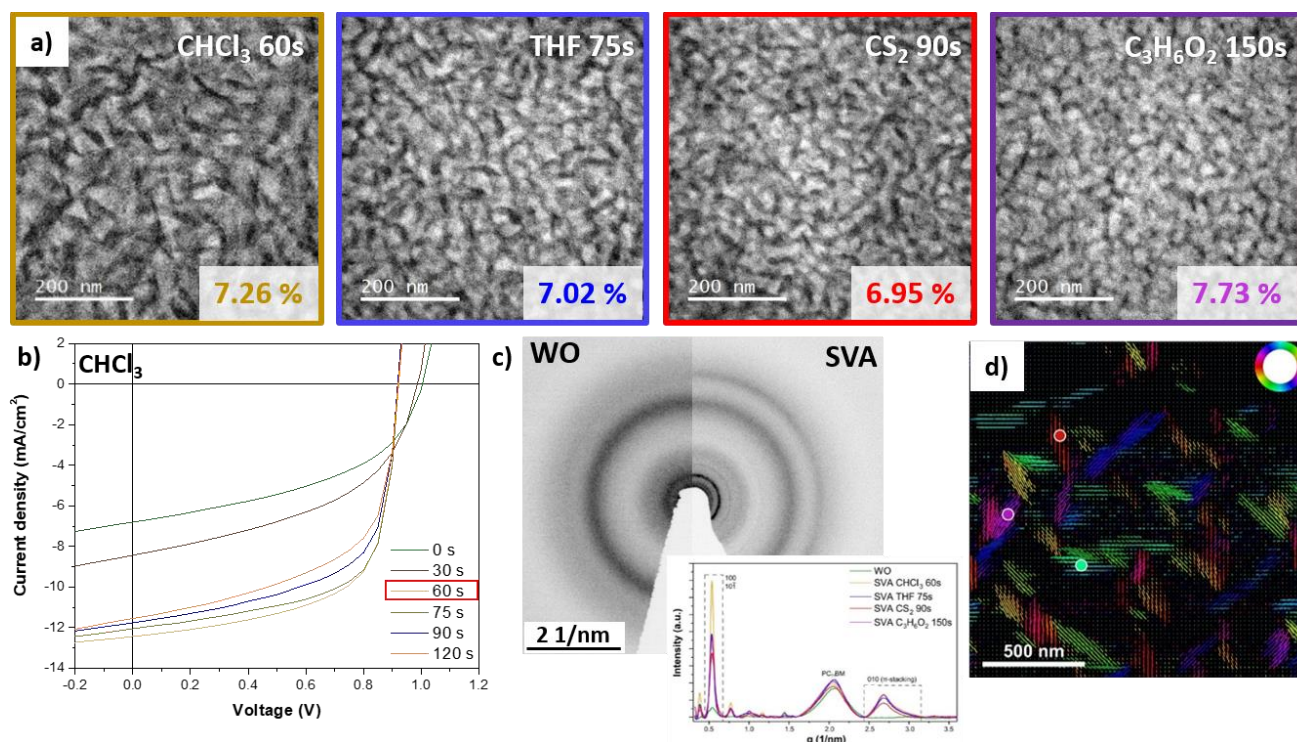
Figure 1. Similar nanomorphologies at optimal annealing times using different solvents for SVA (a), device characteristics as a function of the annealing time for SVA with CHCl3 (b), effects of SVA on the donor crystallinity investigated by EF-ED (c) and crystal orientation of the DRCN5T crystallites within the active layer obtained from diffraction imaging techniques (d).
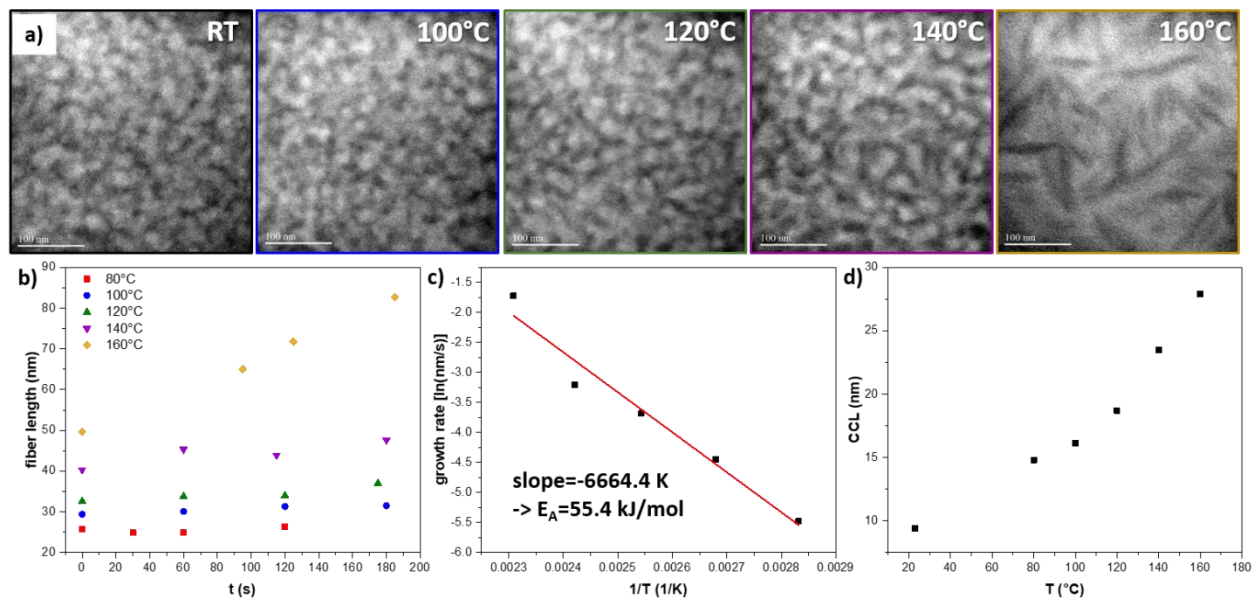
Figure 2. Figure 2: Evolution of the nanomorphology as a function of the annealing temperature (a), plot of the DRCN5T fiber length over time (b) as a basis for the Arrhenius plot in c) and evolution of the crystal coherence length as a function of the annealing temperature (d).

References

[1] G. Yu et al., Science **270** (1995), p. 1789-17991.
[2] J. Min et al., Nano Energy **28** (2016), p. 241-249.
[3] O. Panova et al., Nature Materials **18** (2019), p. 860-865.